Seasonal changes in the D/H ratio of fatty acids of pelagic microorganisms in the coastal North Sea

Sandra Mariam Heinzelmann[#1], Nicole Jane Bale[1], Laura Villanueva[1], Danielle Sinke-Schoen[1], Catharina Johanna Maria Philippart[2,3], Jaap Smede Sinninghe Damsté[1,4], Stefan Schouten[1,4], Marcel Teunis Jan van der Meer[1]

[1] Department of Marine Microbiology and Biogeochemistry, NIOZ Royal Netherlands Institute for Sea Research and Utrecht University, P.O. Box 59, 1790 AB Den Burg, The Netherlands

[2] Department of Coastal Systems Sciences, NIOZ Royal Netherlands Institute for Sea Research and Utrecht University, P.O. Box 59, 1790 AB Den Burg, The Netherlands

[3] Utrecht University, Faculty of Geosciences, Department of Physical Geography, Coastal Processes, P.O. box 80.115, 3508 TC Utrecht, The Netherlands

[4] Utrecht University, Faculty of Geosciences, Department of Earth Sciences, Geochemistry, P.O. Box 80.021, 3508 TA Utrecht, The Netherlands

[#]corresponding author: sandra.m.heinzelmann@gmail.com

Running title: Fatty acid D/H ratio of coastal microbial communities

Keywords: metabolism, fatty acids, photoautotrophs, heterotrophs, algal bloom, 16S rRNA gene amplicon pyrosequencing, bacterial diversity, coastal environment, hydrogen isotopes

Abstract

Culture studies of microorganisms have shown that the hydrogen isotopic composition of fatty acids depends on their metabolism, but there are only few environmental studies available to confirm this observation. Here we studied the seasonal variability of the deuterium/hydrogen (D/H) ratio of fatty acids in the coastal Dutch North Sea and compared this with the diversity of the phyto- and bacterioplankton. Over the year, the stable hydrogen isotopic fractionation factor ε between fatty acids and water ($\varepsilon_{lipid/water}$) ranged between -172 ‰ and -237 ‰, the algal-derived polyunsaturated fatty acid *n*C20:5 generally being the most D-depleted (-177 ‰ to -235 ‰) and *n*C18:0 the least D-depleted fatty acid (-172 ‰ to -210 ‰). The in general highly D-depleted *n*C20:5 is in agreement with culture studies, which indicates that photoautotrophic microorganisms produce fatty acids which are significantly depleted in D relative to water. The $\varepsilon_{lipid/water}$ of all fatty acids showed a transient shift towards increased fractionation during the spring phytoplankton bloom, indicated by increasing chlorophyll *a* concentrations and relative abundance of the *n*C20:5 PUFA, suggesting increased contributions of photoautotrophy. Time periods with decreased fractionation (less negative $\varepsilon_{lipid/water}$ values) can potentially be explained by an increased contribution of heterotrophy to the fatty acid pool. Our results show that the hydrogen isotopic composition of fatty acids is a promising tool to assess the community metabolism of coastal plankton potentially in combination with the isotopic analysis of more specific biomarker lipids.

1. Introduction

The hydrogen isotopic composition of fatty acids of microorganisms has been shown to depend on different factors like metabolism, salinity, biosynthetic pathways, growth phase and temperature (Dirghangi and Pagani, 2013; Fang et al., 2014; Heinzelmann et al., 2015a; Heinzelmann et al., 2015b; Zhang et al., 2009a; Zhang et al., 2009b). While most of these factors lead to relatively small variations in the deuterium to hydrogen (D/H) ratio of fatty acids (10-

20 ‰), differences in the central metabolism of microorganisms have a much more pronounced effect (Zhang et al., 2009a). Both photo- and chemoautotrophs produce fatty acids depleted in D compared to growth water with the stable hydrogen isotopic fractionation factor ε between the *n*C16:0fatty acid, the most commonly occurring fatty acid in microorganisms, and water ($\varepsilon_{lipid/water}$) ranging between -160 ‰ to -220 ‰ and -250 ‰ and -400 ‰, respectively (Campbell et al., 2009; Chikaraishi et al., 2004; Heinzelmann et al., 2015a; Heinzelmann et al., 2015b; Sessions et al., 2002; Valentine et al., 2004; Zhang et al., 2009a; Zhang and Sachs, 2007). In contrast, heterotrophs produce *n*C16:0 fatty acid with either a relatively minor depletion or an enrichment in D compared to the growth water with $\varepsilon_{lipid/water}$ values ranging between -150 ‰ and +200 ‰ (Dirghangi and Pagani, 2013; Fang et al., 2014; Heinzelmann et al., 2015a; Heinzelmann et al., 2015b; Sessions et al., 2002; Zhang et al., 2009a). It has been speculated that the differences in hydrogen isotopic composition of fatty acids produced by organisms expressing different core metabolisms, i.e. heterotrophy and photo- and chemoautotrophy are mainly due to the D/H ratio of the H added to nicotinamide adenine dinucleotide phosphate ($NADP^+$) and the hydrogen isotope fractionation associated with the reduction of $NADP^+$ to NADPH and is used during fatty acid biosynthesis (Zhang et al., 2009a). $NADP^+$ is reduced to NADPH during a number of different reactions in multiple different metabolic pathways (each associated with different hydrogen isotopic fractionations) and is subsequently used as a major source of hydrogen in lipid biosynthesis (Robins et al., 2003; Saito et al., 1980; Schmidt et al., 2003).

Although the metabolism of a microorganism in pure culture is reflected by the D/H ratio of its fatty acids, it is not clear if the D/H ratio of fatty acids from environmental microbial communities can be used to assess the community 'integrated' core metabolisms and changes therein in nature. Culture conditions rarely represent environmental conditions since cultures are typically axenic and use a single substrate, they do not take into account microbial

interactions, which have been shown to affect the hydrogen isotopic composition of lipids (Dawson et al., 2015) and they test a limited number of potential substrates, energy sources and core metabolisms. Previous studies of environmental samples observed a wide range in the D/H ratio of lipids in both the marine water column and sediment (Jones et al., 2008; Li et al., 2009), suggesting inputs of organisms with a variety of metabolisms. Osburn et al. (2011) showed that different microbial communities from various hot springs in Yellowstone National Park produce fatty acids with hydrogen isotopic compositions in line with the metabolism expressed by the source organism. The D/H ratio of specific fatty acids, which could be attributed to microorganisms expressing a specific core metabolism, was within the range expected for that metabolism. On the other hand, the D/H ratio of common or general fatty acids (e.g. *n*C16:0) allowed for assessing the metabolism of the main contributors of these more general fatty acid, but not necessarily the metabolism of the dominant community members (Osburn et al., 2011). These first environmental results indicate the applicability of this new method, and clearly indicates the limitation of looking only at general occurring fatty acids.

Here, we studied the seasonal variability of the hydrogen isotopic composition of fatty acids from coastal North Sea water sampled from the jetty at the Royal Netherlands Institute for Sea Research (NIOZ) in order to examine the relationship between hydrogen isotope fractionation in fatty acids and the general metabolism of the microbial community. Time series studies have been previously performed at the NIOZ jetty to determine phytoplankton and prokaryotic abundances and composition (Alderkamp et al., 2006; Brandsma et al., 2012; Brussaard et al., 1996; Philippart et al., 2010; Philippart et al., 2000; Pitcher et al., 2011; Sintes et al., 2013), lipid composition (Brandsma et al., 2012; Pitcher et al., 2011), and chlorophyll *a* concentration (Philippart et al., 2010). Typically, the spring bloom in the coastal North Sea is predominantly comprised of *Phaeocystis globosa*, followed directly by a bloom of various diatom species, a second moderate diatom bloom of *Thalassiosira* spp. and *Chaetoceros socialis* that occurs in

early summer and an autumn bloom is formed by *Thalassiosira* spp., *C. socialis*, cryptophytes and cyanobacteria (Brandsma et al., 2012; Cadée and Hegeman, 2002). However the autumn bloom seems to have weakened over the last years (Philippart et al., 2010). The abundance of bacteria increases following the algal blooms and the bacteria are dominated by heterotrophs, e.g. bacteria belonging to the *Bacteroidetes* (Alderkamp et al., 2006), using released organic matter from declining phytoplankton blooms as carbon, nitrogen and phosphate sources. The intact polar lipid (IPL) composition of the microbial community was shown to be composed mainly of phospholipids, sulfoquinovosyldiacylglycerol and betaine lipids with a limited taxonomic potential (Brandsma et al., 2012). The main source of those lipids was assumed to be the eukaryotic plankton.

This well studied site should allow us to trace the shift from an environment dominated by photoautotrophs during major phytoplankton blooms, towards an environment with a higher abundance of heterotrophic bacteria following the end of the bloom (Brandsma et al., 2012). These shifts in the community structure should be reflected in the D/H ratio of fatty acids. We, therefore, analysed the D/H ratio of polar lipid derived fatty acids (PLFA) over a seasonal cycle and compared this with phytoplankton composition data and abundance and information on the bacterial diversity obtained by 16S rRNA gene amplicon sequencing.

2. Material and Methods

2.1. Study site and sampling

From September 2010 until December 2011 water samples were taken from the NIOZ sampling jetty in the Marsdiep at the western entrance of the North Sea into the Wadden Sea at the island of Texel (53°00’06” N 4°47’21” E). Surface water samples (depth max ±50 cm below surface) were collected for suspended particulate matter (SPM) biweekly during high tide to ensure that water sampled was from the North Sea.

For lipid analysis measured volumes of water (ca. 9-11 L) were filtered consecutively, without pre filtration, through pre-ashed 3 and 0.7 µm pore size glass fibre filters (GF/F, Whatman; 142 mm diameter) and stored at -20 ºC until lipid extraction. For DNA analysis approximately 1 L seawater was filtered through a polycarbonate filter (0.2 µm pore size; 142 mm diameter; Millipore filters) and stored at -80 ºC until extraction.

Salinity measurements were done during the time of sampling with either an Aanderaa Conductivity/Temperature sensor 3211 connected to an Aanderaa datalogger DL3634 (Aanderaa Data Instruments AS, Norway) or a Refractometer/Salinometer Endeco type 102 handheld (Endeco, USA).

For chlorophyll *a* measurements 500 mL sea water was filtered through a 47 mm GF/F filter (0.7 µm pore size, Whatman, GE Healthcare Life Sciences, Little Chalfont, UK) and immediately frozen in liquid nitrogen. Samples were thawed and homogenised with glass beads and extracted with methanol. Chlorophyll *a* concentration was measured with a Dionex high-performance liquid chromatograph (HPLC) (Philippart et al., 2010).

Water samples for salinity versus δD_{water} calibration (see below) were sampled weekly between March and September 2013 at high tide. Salinity was determined using a conductivity meter (VWR EC300) calibrated to IAPSO standard seawater of salinities 10, 30, 35 and 37.

2.2. Polar lipid derived fatty acids

Filters were extracted for IPLs and eventually fatty acid analysis. The 0.7 µm filters did not yield enough total lipid extract for analysis. Therefore, only fatty acids obtained from the 3 µm filters were analysed. Due to fast clogging of the filters and a corresponding decrease of the pore size (Sørensen et al., 2013), the 3 µm filters will most likely contain most of the microorganisms present in North Sea water, although it cannot be excluded that the microorganisms retained on the filter are biased towards a larger cell size. Freeze dried filters

were extracted via a modified Bligh-Dyer method (Bligh and Dyer, 1959; Rütters et al., 2002) with methanol (MeOH)/dichloromethane (DCM)/phosphate buffer (2:1:0.8, vol/vol/vol) using ultrasonication (Heinzelmann et al., 2014). Approximately 0.5 - 1 mg of the Bligh-Dyer extract (BDE) was separated into a neutral and polar lipid fraction using silica column chromatography (Heinzelmann et al., 2014). The BDE was added onto a DCM pre-rinsed silica column (0.5 g; activated for 3 h at 150°C) and eluted with 7 mL of DCM and 15 mL of MeOH. The resulting fractions were dried under nitrogen and stored at -20 °C. PLFAs were obtained via saponification of the MeOH fraction with 1 N KOH in MeOH (96%). The samples were refluxed at 140 °C for 1 h. Afterwards the pH was adjusted to 5 with 2 N HCl/MeOH (1/1), bidistilled H_2O and DCM were added. The MeOH/H_2O layer was washed twice with DCM, the DCM layers were combined and water removed using Na_2SO_4. The sample was dried under nitrogen and stored in the fridge. The PLFAs were methylated with boron trifluoride-methanol (BF_3-MeOH) for 5 min at 60 °C. Afterwards H_2O and DCM were added. The H_2O/MeOH layer was washed three times with DCM, and potential traces of water were removed over a small Na_2SO_4 column after which the DCM was evaporated under a stream of nitrogen. In order to obtain a clean PLFA fraction for isotope analysis, the methylated extract was separated over an aluminium oxide (Al_2O_3) column, eluting the methylated PLFAs with three column volumes of DCM. For identification of the position of double bonds in unsaturated fatty acids, the methylated PLFAs were derivatised with dimethyldisulfide (DMDS) (Nichols et al., 1986). Hexane, DMDS and I_2/ether (60 mg/mL) were added to the fatty acids and incubated at 40 °C overnight. After adding hexane, the iodine was deactivated by addition of a 5% aqueous solution of $Na_2S_2O_3$. The aqueous phase was washed twice with hexane. The combined hexane layers were cleaned over Na_2SO_4 and dried under a stream of nitrogen. The dried extracts were stored at 4 °C.

2.3. Fatty acid and hydrogen isotope analysis

The fatty acid fractions were analysed by gas chromatography (GC) using an Agilent 6890 GC with a flame ionization detector (FID) using a fused silica capillary column (25 m x 320 µm) coated with CP Sil-5 (film thickness 0.12 µm) with helium as carrier gas. The temperature program was as follows: initial temperature 70 °C, increase of temperature to 130 °C with 20 °C min^{-1}, and then to 320 °C with 4 °C min^{-1} which was kept for 10 min. Individual compounds and double bond positions (see above) were identified using GC/mass spectrometry (MS) (Schouten et al., 1998).

Hydrogen isotope analysis of the fatty acid fraction was performed by GC thermal conversion (TC) isotope ratio monitoring (ir) MS using an Agilent 7890 GC connected via Thermo GC Isolink and Conflo IV interfaces to a Thermo Delta V MS according to Chivall et al. (2014). Samples were injected onto an Agilent CP-Sil 5 CB column (25 m × 0.32 mm ID; 0.4 µm film thickness; He carrier gas, 1.0 mL min^{-1}). The GC temperature program was 70 °C to 145 °C at 20 °C min^{-1}, then to 320 °C at 4 °C min^{-1} where it was kept for 15 min. Eluting compounds were converted to H_2 at 1420°C in an Al_2O_3 tube before introduction into the mass spectrometer. The H^{3+} correction factor was determined daily and was constant at 5.3±0.2. A set of standard *n*-alkanes with known isotopic composition (Mixture B prepared by Arndt Schimmelmann, University of Indiana) was analyzed daily prior to analyzing samples in order to monitor the system performance. Samples were only analyzed when the n-alkanes in Mix B had an average deviation from their off-line determined value of <5 ‰. An internal standard, squalane (δD = -170 ‰) was co-injected with each fatty acid sample fraction in order to monitor the accuracy of the measurements over time with δD = -164±4 ‰. The δD of the individual fatty acids was measured in duplicates and corrected for the added methyl group (Heinzelmann et al., 2015b). δD of water samples was determined by elemental analysis (EA)/TC/irMS according to Chivall et al. (2014).

2.4. Phytoplankton abundance and diversity

Phytoplankton samples were preserved with acid Lugol's iodine, and cells were counted with a Zeiss inverted microscope using 3 mL counting chambers. Most photoautotrophic microorganisms were identified to species level, but some were clustered into taxonomic and size groups (Philippart et al., 2000). For each sampling date in the period from September 2010 to December 2011, the densities of the most abundant phytoplankton species or species' groups were calculated. The three most dominant phytoplankton species (or groups) together comprised, on average, more than 60% of the total numbers of marine phytoplankton in the Marsdiep during this study period.

2.5. DNA extraction

The 0.2 µm polycarbonate filters were defrosted and cut into small pieces with sterile scissors and then transferred into a 50 mL falcon tube. Filter pieces were lysed by bead-beating with ~1 g of sterile 0.1 mm zirconium beads (Biospec, Bartlesville, OK) in 10 mL RLT buffer (Qiagen) and 100 µL β-mercaptoethanol for 10 min. 1/60 volume RNase A (5 µg/µL) was added to the lysate, incubated for 30 min at 37 ºC and afterwards cooled down for 5 min on ice. The lysate was purified with the DNeasy Blood and Tissue kit (Qiagen, Hilden). DNA was eluted with 3x 100 µL AE buffer, the eluates pooled and reconcentrated. DNA quality and concentration was estimated by Nanodrop (Thermo Scientific, Waltham, MA) quantification.

2.6. 16S rRNA gene amplicon sequencing and analysis

The general bacterial diversity was assessed by 16S rRNA gene amplicon pyrotag sequencing. The extracted DNA was quantified fluorometrically with Quant-iT^{TM} PicoGreen® dsDNA Assay Kit (Life Technologies, The Netherlands).

PCR reactions were performed with the universal (Bacteria and Archaea) primers S-D-Arch 0519-a-S-15 (5'-CAG CMG CCG CGG TAA-3') and S-D-Bact-785-a-A-21 (5'-GAC TAC HVG GGT ATC TAA TCC-3') (Klindworth et al., 2012) adapted for pyrosequencing by the addition of sequencing adapters and multiplex identifier (MID) sequences. To minimize bias three independent PCR reactions were performed containing: 16.3 µL H_2O, 6 µL HF Phusion buffer, 2.4 µL dNTP (25 mM), 1.5 µL forward and reverse primer (10 µM; each containing an unique MID tail), 0.5 µL Phusion Taq and 2 µL DNA (6 ng/µL). The PCR conditions were following: 98 ºC, 30 s; 25× [98 ºC, 10 s; 53 ºC, 20 s; 72 ºC, 30 s]; 72 ºC, 7 min and 4 ºC, 5 min.

The PCR products were loaded on a 1% agarose gel and stained with SYBR® Safe (Life Technologies, The Netherlands). Bands were excised with a sterile scalpel and purified with Qiaquick Gel Extraction Kit (QIAGEN, Valencia, CA) following the manufacturer's instructions. PCR purified products were quantified with Quant-iT^{TM} PicoGreen® dsDNA Assay Kit (Life Technologies, The Netherlands). Equimolar concentrations of the barcoded PCR products were pooled and sequenced on GS FLX Titanium platform (454 Life Sciences) by Macrogen Inc. Korea.

Samples were analyzed using the QIIME pipeline (Caporaso et al., 2010). Raw sequences were demultiplexed and then quality-filtered with a minimum quality score of 25, length between 250−350 bp, and allowing maximum two errors in the barcode sequence. Sequences were then clustered into operational taxonomic units (OTUs, 97% similarity) with UCLUST (Edgar, 2010). Reads were aligned to the Greengenes Core reference alignment (DeSantis et al., 2006) using the PyNAST_algorithm (Caporaso et al., 2010). Taxonomy was assigned based on the Greengenes taxonomy and a Greengenes reference database (version 12_10) (McDonald et al., 2012; Werner et al., 2012). Representative OTU sequences assigned to the specific taxonomic groups were extracted through classify.seqs and get.lineage in Mothur (Schloss et al., 2009) by using the Greengenes reference and taxonomy files. The 16S rRNA gene amplicon reads (raw

data) have been deposited in the NCBI Sequence Read Archive (SRA) under BioProject number PRJNA293285.

2.7. Phylogenetic analyses

The phylogenetic affiliation of the 16S rRNA gene sequences was compared to release 119 of the Silva NR SSU Ref database (http://www. arb-silva.de/; Quast, 2012) using the ARB software package (Ludwig et al., 2004). Sequences were added to the reference tree supplied by the Silva database using the ARB Parsimony tool.

3. Results

3.1. Chlorophyll *a* concentration and phytoplankton abundance and diversity

Chlorophyll *a* concentrations ranged between 0.4 and 22.2 µg L^{-1} (Fig. 1; Table S1). During late autumn, winter and early spring concentrations were low at ~4 µg L^{-1}. A peak in the chlorophyll *a* concentration occurred in the beginning of April and values stayed relatively high during this month, indicative of the spring bloom. Subsequently, the chlorophyll *a* concentration decreased again, reaching pre-bloom levels and stayed relatively constant thereafter.

Phytoplankton diversity and abundance was determined using light microscopy and the two to three most abundant phytoplankton species were identified and counted (Table S2). The majority of the phytoplankton was composed of *Phaeocystis globosa*, diatoms and cyanobacteria (Fig. 2), with the spring bloom primarily being made up of *P. globosa*. The highest abundance of diatoms was also during spring, while the cyanobacteria reached the highest abundance in the beginning of the sampling period from autumn until late winter and again during summer.

3.2. Bacterial diversity

To assess bacterial diversity, 16S rRNA gene amplicon sequencing was performed on approximately half of the SPM samples (Table S3a+b).

The bacteria detected consisted mainly of members of *Actinobacteria*, *Bacteriodetes*, *Planctomycetes*, *α-Proteobacteria*, *β-Proteobacteria*, *γ-Proteobacteria* and *Verrucomicrobia* (Fig. 3; Table S3a). The majority of the reads belonged to the orders of the *Flavobacteriales*, *Rhodobacteriales*, *Rickettsiales*, *Alteromonadales* and *Oceanospirillales*. The *Flavobacteriales* clade were one of the main contributors (12 to 32 %) to the total bacteria reads with a maximum from beginning of April until the end of May. The percentage of reads attributed to the *Flavobacteriales* decreased during summer and early autumn. Sequence reads affiliated to the *Rhodobacteriales* (6 to 12 %) and *Rickettsiales* (3 to 17 %) were the most represented within the *α-Proteobacteria*. *Alteromonadales* reads made up between 9 and 17 % of all bacteria reads and the percentage of *Oceanospirillales* reads were between 3 and 12 % of the total bacteria reads (Fig. 3; Table S3b).

For a more accurate taxonomic classification of the bacterial groups, sequence reads of the *Bacteriodetes*, *α-Proteobacteria* and *γ-Proteobacteria* were extracted from the dataset and a phylogenetic tree was constructed (Fig. S1-S3a+b). Within the *Flavobacteriales* (*Bacteroidetes*) the majority of the reads fell either within the *Cryomorphaceae* or the *Flavobacteriaceae* with sequences clustering within *Fluviicola* and *Crocinitomix*, *Flavobacterium* and *Tenacibaculum*, respectively. Within the *Rhodobacterales* (*α-Proteobacteria*) most of the reads belonged to *Rhodobacteraceae* and sequences within this family were closely related to the genus *Octadecabacter*. Within the *Rickettsiales* most of the reads were affiliated to the *Pelagibacteraceae* (SAR11 cluster). The majority of the *γ-Proteobacteria* reads were classified within the *Alteromonadales* and *Oceanospirillales*. The

286 *Alteromonadales* reads and sequences fell within the linage of the uncultured *HTCC2188*-
287 isolate and *OM60*-clade and various members of the *Alteromonadaceae*-family. The
288 *Halomonadaceae* family comprised most of the *Oceanospirillales* reads and additionally
289 sequences clustered with various members of the *Oceanospirillaceae*.

290 **3.3. Fatty acid distribution in North Sea SPM**

291 Polar lipid derived fatty acids were comprised of *n*C14:0, *n*C16:1ω7, *n*C16:0, *n*C18:0, the
292 polyunsaturated fatty acid (PUFA) *n*C20:5, and various unsaturated *n*C18 fatty acids (Fig. 4;
293 Table S4). The *n*C14:0 fatty acid followed a seasonal cycle with the lowest relative abundance
294 during winter, and the highest from June to August (Fig. 4a). The *n*C16:0 fatty acid was the
295 dominant fatty acid (21-38 %) with no clear seasonal pattern (Fig. 4c). The *n*C16:1 fatty acid
296 was the next most abundant fatty acid (13–35 %) with a maximum from March to April (Fig.
297 4b). Various unsaturated *n*C18:x fatty acids were observed throughout the season. Due to low
298 abundance of the individual fatty acids and co-elutions the double bond positions could not be
299 determined. These unsaturated fatty acids made up 9–30 % of all fatty acids (Fig. 4d). The
300 *n*C18:0 fatty acid had relative abundances varying between 2–18 % with the highest relative
301 abundance during autumn months (10–18 %) and the lowest during spring, 2–6 % (Fig. 4e). A
302 *n*C20:5 PUFA (Fig. 4f) was observed in most samples with the highest relative abundance
303 during March and April (11–14 %) and early August (18 %). Trace amounts of *n*C15:0, *i*C15:0
304 and *ai*C15:0 fatty acids were also detected.

305 **3.4. Hydrogen isotopic composition of fatty acids**

306 δD values of *n*C14:0, *n*C16:1ω7, *n*C16:0, *n*C18:0 and *n*C20:5 fatty acids were obtained for most
307 of the samples (Table S5). The D/H ratio of the other fatty acids could not be determined with
308 sufficient accuracy due to either incomplete separation or low abundance.

In general, *n*C14:0 and *n*C20:5 were the most depleted fatty acids with δD values ranging between -198 to -241 ‰ and -180 to -241 ‰, respectively. The *n*C18:0 was typically the fatty acid with the highest δD values ranging between -175 to -212 ‰ (Table S5).

4. Discussion

4.1. Hydrogen isotopic fractionation expressed in fatty acids

For the proper assessment of the impact of metabolism on the hydrogen isotopic composition of fatty acids the hydrogen isotopic fractionation of the fatty acids versus water is required ($\varepsilon_{lipid/water}$). For this, the δD of the water (δD_{water}) at the time of sampling is needed. However, at the time of sampling of the SPM unfortunately no water samples were taken and preserved for δD analysis. Therefore, we used an alternative approach to estimate δD_{water} using the salinity of the water measured at the time of sampling. A strong correlation between salinity and δD_{water} is generally observed in marine environments since both parameters depend on evaporation, precipitation and freshwater influx (Craig and Gordon, 1965; Mook, 2001). To establish a local salinity - δD_{water} correlation, water samples were collected weekly during high tide (March to September 2013) and salinity and δD_{water} were measured. Indeed, a strong correlation between salinity and δD_{water} is observed (R^2=0.68; Fig. S4). Using this correlation and the salinities measured, we reconstructed δD_{water} values at the time of sampling of the biomass (Table 1). The error in the estimate of δD_{water} values resulting from this approach is approximately 1.5 ‰, which is less than the error in the determination of δD of the fatty acids (1-12 ‰) and minor compared to the entire range in fatty acid δD (-174 to -241 ‰) and $\varepsilon_{lipid/water}$ (-173 to -237 ‰).

All fatty acids were depleted in D compared to water with the fractionation factor $\varepsilon_{lipid/water}$ ranging from -173 to -237 ‰, all following a similar seasonal trend with the highest degree of fractionation during spring to early summer, and early autumn (Fig. 5; Table 1). The lowest

degree of fractionation (most positive $\varepsilon_{lipid/water}$ values) was in general during late autumn and the winter months.

4.2. Source affects the hydrogen isotopic composition of individual fatty acids

The *n*C20:5 PUFA is the most specific fatty acid detected in North Sea SPM and is exclusively produced by algae (Carrie et al., 1998). Here the *n*C20:5 PUFA is generally one of the most D-depleted fatty acids (Fig. 5), which is in agreement with culture studies that show that photoautotrophic microorganisms produce fatty acids that are depleted in D with $\varepsilon_{lipid/water}$ values between -160 and -220 ‰ (Heinzelmann et al., 2015b and references therein), while heterotrophic microorganisms on the other hand produce fatty acids with $\varepsilon_{lipid/water}$ values ranging between -150 to +200 ‰ (Heinzelmann et al., 2015b and references therein). Furthermore, its concentration increased at the time of the phytoplankton bloom (Fig. 4). Interestingly, after the phytoplankton bloom, when the abundance of pelagic algae had decreased (Fig. 4), it became more enriched in D (Fig. 5). This enrichment might be due to changes in the relative contribution of source organisms. In diatoms *n*C20:5 PUFA can be one of the most abundant fatty acids, while *Phaeocystis* produces it in minor amounts only (Table S6). During the spring bloom both organisms will contribute to the fatty acid pool, while afterwards diatoms are the main source (Fig. 2; Table S2). A changing contribution from different species could potentially affect the hydrogen isotopic composition of a fatty acid even if the source organisms are all photoautotrophic phytoplankton. For instance, colony forming algae such as *Eudorina unicocca* and *Volvox aureus*, have been shown to fractionate much less against D than other algae (Zhang et al., 2007; Heinzelmann et al., 2015b). Indeed, *Phaeocystis*, although belonging to a different phylum, is also a colony forming algae. However, if this would be the reason for the changing D content of the *n*C20:5 PUFA following the spring bloom it would then be expected to become more D depleted with a reduced contribution from *Phaeocystis*, not a D enriched. A potential reason for the relatively D enriched *Phaeocystis*

lipids could be excretion of large amounts of D depleted organic matter, leading directly or indirectly, through the isotopic composition of cell water, to D enriched lipids (Sachs et al., 2016), as has been observed for colony forming algae. Increased organic matter excretion by phytoplankton at the end of the bloom could therefore be another mechanism explaining the D enrichment of the *n*C20:5 PUFA. Another possible reason could be that after the bloom and due to nutrient limitation, phytoplankton hypothetically might use more storage products potentially leading to an increased production of NADPH via other pathways than photosynthesis. The NADPH produced by photoautotrophs via photosystem I is depleted in D (Zhang et al., 2009a), while NADPH produced via the pentose phosphate (OPP) pathway and the tricarboxylic acid (TCA) cycle is relatively enriched in D (Heinzelmann et al., 2015b; Zhang et al., 2009a). The utilization of storage products would lead to an increased reduction of $NADP^+$ to NADPH via both the OPP pathway and the TCA cycle leading to more positive $\varepsilon_{lipid/water}$ values of the *n*C20:5 PUFA after the bloom. In batch culture with increasing nutrient limitation fatty acids of algae became enriched in D with increasing age of the culture (Heinzelmann et al., 2015b) potentially due to a shift in the origin of NADPH or the excretion of organic matter or a combination of multiple factors.

Of all other fatty acids *n*C14:0 was generally the most D-depleted fatty acid, possibly suggesting a higher contribution of photoautotrophic organisms to this fatty acid. However, it has be reported that fatty acids in general seem to become more enriched in D with chain length both in cultures and in environmental samples which might play a minor role here as well (Jones et al., 2008; Campbell et al., 2009; Osburn et al., 2011). The quite similar $\varepsilon_{lipid/water}$ values of *n*C16:0 (-179 to -224 ‰) and *n*C16:1 (-173 to -215 ‰) suggest similar sources for the two fatty acids. The least negative $\varepsilon_{lipid/water}$ values for *n*C18:0 suggest that the sources of this fatty acid might differ from the other fatty acids i.e. with a higher contribution of heterotrophs compared to the other fatty acids. Alternatively, as discussed above fatty acids become more enriched in

382 D with increasing chain length both in cultures and environmental samples (Jones et al., 2008;
383 Campbell et al., 2009; Osburn et al., 2011) which could be part of the reason why the *n*C18:0
384 is relatively enriched in D.

385 Fatty acids profiles of representatives of most members of the phytoplankton and bacterial
386 community observed at our site have been previously reported (Table S6) and can be used to
387 assess the main sources of the different fatty acid pools. The main bacterial contributors to the
388 *n*C16:0 and *n*C16:1ω7 fatty acids are most likely members of the *Alteromonadales* and the
389 *Halomonadaceae,* while the majority of bacterial contributors to the *n*C14:0 and *n*C18:0 fatty
390 acid are derived from the *Puniceicoccales* (Table S6). Both the *Flavobacteriales* and the
391 *Rhodobacteriaceae,* which make up a large part of the total bacteria reads, will hardly contribute
392 to the measured isotopic signal as they have been reported to produce only traces of *n*C14:0,
393 *n*C16:0, *n*C16:1ω7 or *n*C18:0 fatty acids (Table S6). The observed phytoplankton species are
394 main contributors to the *n*C14:0, *n*C16:0 and *n*C16:1ω7 fatty acid pools, but contribute
395 relatively little to the *n*C18:0 fatty acid pools. *Phaeocystis* produces mainly the *n*C14:0 and
396 *n*C16:0 fatty acids (Hamm and Rousseau, 2003; Nichols et al., 1991).

397 Overall, the majority of the *n*C14:0 fatty acid pool will likely be predominately derived from
398 photoautotrophs (Table S6), which potentially explains why the *n*C14:0 is almost always the
399 most depleted fatty acid. The *n*C18:0 fatty acid on the other hand, will be largely derived from
400 heterotrophic bacteria (Table S6) resulting in more D enriched signal compared to that of the
401 *n*C14:0 fatty acid. However, the hydrogen isotopic composition of the *n*C18:0 fatty acid still
402 falls within the range for photoautotrophic organisms, albeit at the higher end, suggesting that
403 although it is only produced in minor amounts by phytoplankton, a relatively high abundance
404 of phytoplankton could still determine its isotopic composition.

None of the fatty acids measured in the North Sea SPM have $\varepsilon_{lipid/water}$ values which fall in the range of those predicted for chemoautotrophs (-264 to -345 ‰; Heinzelmann et al., 2015b and references therein). This fits with the observation that sequence reads of chemoautotrophic bacteria accounted for < 3 % of the total bacterial reads (Fig. 3; Table S3a+b), and thus it is unlikely that this metabolism plays an important role in this environment.

4.3. Linking seasonal changes of hydrogen isotope fractionation to changes in community metabolism

In general most fatty acids showed a similar seasonal trend with the most negative ε values in spring and the most positive ε values in the winter (Fig. 5). In order to assess the dominant metabolism of the whole microbial community we calculated a weighted average ε of all measured fatty acids apart from the specific *n*C20:5 PUFA. The weighted average $\varepsilon_{lipid/water}$ ($\varepsilon_{\Sigma FA}$) followed the same seasonal trend as the $\varepsilon_{lipid/water}$ values of the individual fatty acids (Fig. 1+5), and ranged between -180 and -225 ‰ with an average of -199 ‰.

Compared to the chlorophyll *a* concentration, the $\varepsilon_{\Sigma FA}$ followed an opposite seasonal trend i.e. when the chlorophyll *a* concentration increased in early April, $\varepsilon_{\Sigma FA}$ decreased (Fig. 5). The chlorophyll *a* maximum in April-May indicates a spring bloom (Fig. 1), which is known to occur annually in North Sea coastal waters (Brandsma et al., 2012; Philippart et al., 2010) and corresponds with a shift towards more negative values for $\varepsilon_{\Sigma FA}$, as well as a high abundance of the algal-derived *n*C20:5 PUFA (Fig. 4). It is likely that at least during the spring bloom the majority of the fatty acids are derived from the dominant algae, i.e. *Phaeocystis* and diatoms, which make up the majority of the bloom, leading to a D depleted signal. Thus, the observation that the value of $\varepsilon_{\Sigma FA}$ was more negative during the spring bloom when the environment is dominated by photoautotrophic microorganisms (Fig. 3) fits with an increased contribution by photoautotrophs relative to heterotrophic microorganisms to the fatty acid pool. At the end of

the bloom more positive $\varepsilon_{\Sigma FA}$ values were observed, which is in agreement with an increased abundance of heterotrophic bacterioplankton in previous studies (Sintes et al., 2013), living on released organic material (Alderkamp et al., 2006). This fits well with previous observations by Brandsma et al. (2012) who studied both the phytoplankton and bacterial communities during a period of twelve months. Cell counts contained in their study showed that the bacterial cell counts were lowest during the spring bloom, increased right after and stayed more or less stable throughout the rest of the sampling period. Phytoplankton cell counts on the other hand were highest during the bloom and dropped extremely afterwards with only the cyanobacteria cell counts increasing slightly in late summer/early autumn. At the same time they showed that in general the bacteria cell count was ten times higher than the phytoplankton cell count. This suggests that the whole environment after the bloom might be dominated by heterotrophic bacteria. The relative stability of the system throughout the last decades (Philippart et al., 2000) suggests that the situation might have been similar during the sampling period described here.

Thus, $\varepsilon_{\Sigma FA}$ values reflect a mixed signal derived from mainly photoautotrophic and, to a lesser extent, heterotrophic microorganisms. Nevertheless, $\varepsilon_{lipid/water}$ values for all fatty acids remain in the range of photoautotrophic metabolism (Heinzelmann et al., 2015b and references therein), indicating that, overall, the fatty acids in this coastal seawater are mostly derived from phototrophic organisms. This is in accordance with the assumption that IPLs (containing fatty acids) in coastal North Sea waters over the annual cycle were predominantly derived from phytoplankton (Brandsma et al., 2012). Our results show that it is possible to study whole community core metabolism in a natural environment by determining the weighted average D/H ratio of all fatty acids.

5. Conclusion

A seasonal study of fatty acids derived from the coastal Dutch North Sea shows that all fatty acids are depleted in D with δD ranging between -174 and -241 ‰. The most negative values were observed during the spring bloom, when the biomass is dominated by photoautotrophic microorganisms. The subsequent higher relative contribution of heterotrophs to the general fatty acid pools leads to shift in $\varepsilon_{lipid/water}$ towards more positive values by up to 20 ‰. This shift towards more positive values is in agreement with observations from culture studies where heterotrophic organisms fractionate much less or even opposite to photoautotrophic organisms, although we cannot exclude the possibility of nutrient limitation affecting phytoplankton growth, leading to a shift in NADPH origin or excretion of organic matter, for instance, which could also affect the hydrogen isotope signal. This study confirms that hydrogen isotopic fractionation as observed in general fatty acids can be used to study the core metabolism of complex environments and to track seasonal changes therein. The combination of hydrogen isotope analysis of general fatty acids with those of more specific biomarker lipids might help further improve the assessment of core metabolisms in present and past environments.

Data availability

Data is available on Pangea under doi:10.1594/PANGAEA.859031

Author Contribution

N.J. Bale helped by providing samples and helped with sampling; L. Villanueva helped with carrying out sequencing experiments and analysis of subsequent data; D. Sinke-Schoen helped with measuring the hydrogen isotopic composition of North Sea water samples; C. J. M. Philippart provided chlorophyll *a* and phytoplankton data; J. S. Sinninghe Damsté, S. Schouten and M. T. J. van der Meer helped design experiments and contributed to the manuscript as

supervisors of S.M. Heinzelmann; S.M. Heinzelmann prepared the manuscript with contributions of all co-authors.

Acknowledgment

The authors would like to thank the editor, Alex Sessions and the two anonymous reviewers for their constructive comments. We thank also Y. A. Lipsewers, E. Svensson and K. K. Sliwinska for their help with sampling, E. Wagemaakers for providing salinity data, M. Veenstra and A. van den Oever for assistance with the phytoplankton sampling and analyses, and M. Verweij for assistance with the GC-MS measurements.. MvdM was funded by the Dutch Organisation for Scientific Research (NWO) through a VIDI grant.

References

Alderkamp, A. C., Sintes, E., and Herndl, G. J.: Abundance and activity of major groups of prokaryotic plankton in the coastal North Sea during spring and summer, Aquat. Microb. Ecol., 45, 237-246, 10.3354/ame045237, 2006.

Bligh, E. G., and Dyer, W. J.: A rapid method of total lipid extraction and purification, Can J Biochem Physiol, 37, 911-917, 10.1139/o59-099, 1959.

Brandsma, J., Hopmans, E. C., Philippart, C. J. M., Veldhuis, M. J. W., Schouten, S., and Sinninghe Damsté, J. S.: Low temporal variation in the intact polar lipid composition of North Sea coastal marine water reveals limited chemotaxonomic value, Biogeosciences, 9, 1073-1084, 10.5194/bg-9-1073-2012, 2012.

Brussaard, C. P. D., Gast, G. J., van Duyl, F. C., and Riegman, R.: Impact of phytoplankton bloom magnitude on a pelagic microbial food web, Mar Ecol Prog Ser, 144, 211-221, 10.3354/meps144211, 1996.

Cadée, G. C., and Hegeman, J.: Phytoplankton in the Marsdiep at the end of the 20th century; 30 years monitoring biomass, primary production, and Phaeocystis blooms, J Sea Res, 48, 97-110, 10.1016/S1385-1101(02)00161-2, 2002.

Campbell, B. J., Li, C., Sessions, A. L., and Valentine, D. L.: Hydrogen isotopic fractionation in lipid biosynthesis by H_2-consuming *Desulfobacterium autotrophicum*, Geochim Cosmochim Ac, 73, 2744-2757, 10.1016/j.gca.2009.02.034, 2009.

Caporaso, J. G., Kuczynski, J., Stombaugh, J., Bittinger, K., Bushman, F. D., Costello, E. K., Fierer, N., Pena, A. G., Goodrich, J. K., Gordon, J. I., Huttley, G. A., Kelley, S. T., Knights, D., Koenig, J. E., Ley, R. E., Lozupone, C. A., McDonald, D., Muegge, B. D., Pirrung, M., Reeder, J., Sevinsky, J. R., Turnbaugh, P. J., Walters, W. A., Widmann, J., Yatsunenko, T., Zaneveld, J., and Knight, R.: QIIME allows analysis of high-throughput community sequencing data, Nat Methods, 7, 335-336, 10.1038/nmeth.f.303, 2010.

Chikaraishi, Y., Suzuki, Y., and Naraoka, H.: Hydrogen isotopic fractionations during desaturation and elongation associated with polyunsaturated fatty acid biosynthesis in marine macroalgae, Phytochemistry, 65, 2293-2300, 10.1016/j.phytochem.2004.06.030, 2004.

Chivall, D., M'Boule, D., Sinke-Schoen, D., Sinninghe Damsté, J. S., Schouten, S., and van der Meer, M. T. J.: The effects of growth phase and salinity on the hydrogen isotopic composition of alkenones produced by coastal haptophyte algae, Geochim Cosmochim Ac, 140, 381-390, 10.1016/j.gca.2014.05.043, 2014.

Craig, H., and Gordon, L. I.: Deuterium and oxygen 18 variations in the ocean and the marine atmosphere, in: Stable Isotopes in Oceanographic Studies and Paleotemperatures, edited by: Tongiogi, E., Consiglio Nazionale Delle Ricerche, Laboratorio Di Geologia Nucleare, Pisa, 9-130, 1965.

520 Dawson, K. S., Osburn, M. R., Sessions, A. L., Orphan, V. J.: Metabolic associations with
521 archaea drive shifts in hydrogen isotopic fractionation in sulfate-reducing bacterial lipids in
522 cocultures and methane seeps, Geobiology, 13.5, 462-477, 10.1111/gbi.12140, 2015
523 DeSantis, T. Z., Hugenholtz, P., Larsen, N., Rojas, M., Brodie, E. L., Keller, K., Huber, T.,
524 Dalevi, D., Hu, P., and Andersen, G. L.: Greengenes, a chimera-checked 16S rRNA gene
525 database and workbench compatible with ARB, Appl Environ Microbiol, 72, 5069-5072,
526 10.1128/aem.03006-05, 2006.
527 Dirghangi, S. S., and Pagani, M.: Hydrogen isotope fractionation during lipid biosynthesis by
528 *Tetrahymena thermophila*, Org Geochem, 64, 105-111, 10.1016/j.orggeochem.2013.09.007,
529 2013.
530 Edgar, R. C.: Search and clustering orders of magnitude faster than BLAST, Bioinformatics,
531 26, 2460-2461, 10.1093/bioinformatics/btq461, 2010.
532 Fang, J., Li, C., Zhang, L., Davis, T., Kato, C., and Bartlett, D. H.: Hydrogen isotope
533 fractionation in lipid biosynthesis by the piezophilic bacterium *Moritella japonica* DSK1, Chem
534 Geol, 367, 34-38, 10.1016/j.chemgeo.2013.12.018, 2014.
535 Hamm, C. E., and Rousseau, V.: Composition, assimilation and degradation of Phaeocystis
536 globosa-derived fatty acids in the North Sea, J Sea Res, 50, 271-283, 10.1016/s1385-
537 1101(03)00044-3, 2003.
538 Heinzelmann, S. M., Bale, N. J., Hopmans, E. C., Sinninghe Damsté, J. S., Schouten, S., and
539 van der Meer, M. T. J.: Critical assessment of glyco- and phospholipid separation by using silica
540 chromatography, Appl Environ Microbiol, 80, 360-365, 10.1128/aem.02817-13, 2014.
541 Heinzelmann, S. M., Chivall, D., M'Boule, D., Sinke-Schoen, D., Villanueva, L., Damsté, J. S.
542 S., Schouten, S., and van der Meer, M. T. J.: Comparison of the effect of salinity on the D/H
543 ratio of fatty acids of heterotrophic and photoautotrophic microorganisms, FEMS Microbiol
544 Lett, 362, 10.1093/femsle/fnv065, 2015a.

Heinzelmann, S. M., Villanueva, L., Sinke-Schoen, D., Sinninghe Damsté, J. S., Schouten, S., and van der Meer, M. T. J.: Impact of metabolism and growth phase on the hydrogen isotopic composition of microbial fatty acids, Front Microbiol, 6, 1-11, 10.3389/fmicb.2015.00408, 2015b.

Jones, A. A., Sessions, A. L., Campbell, B. J., Li, C., and Valentine, D. L.: D/H ratios of fatty acids from marine particulate organic matter in the California Borderland Basins, Org Geochem, 39, 485-500, 10.1016/j.orggeochem.2007.11.001, 2008.

Klindworth, A., Pruesse, E., Schweer, T., Peplies, J., Quast, C., Horn, M., and Glöckner, F. O.: Evaluation of general 16S ribosomal RNA gene PCR primers for classical and next-generation sequencing-based diversity studies, Nucleic Acids Res, 10.1093/nar/gks808, 2012.

Li, C., Sessions, A. L., Kinnaman, F. S., and Valentine, D. L.: Hydrogen-isotopic variability in lipids from Santa Barbara Basin sediments, Geochim Cosmochim Ac, 73, 4803-4823, 10.1016/j.gca.2009.05.056, 2009.

Ludwig, W., Strunk, O., Westram, R., Richter, L., Meier, H., Yadhukumar, Buchner, A., Lai, T., Steppi, S., Jobb, G., Förster, W., Brettske, I., Gerber, S., Ginhart, A. W., Gross, O., Grumann, S., Hermann, S., Jost, R., König, A., Liss, T., Lüßmann, R., May, M., Nonhoff, B., Reichel, B., Strehlow, R., Stamatakis, A., Stuckmann, N., Vilbig, A., Lenke, M., Ludwig, T., Bode, A., and Schleifer, K. H.: ARB: a software environment for sequence data, Nucleic Acids Res, 32, 1363-1371, 10.1093/nar/gkh293, 2004.

McDonald, D., Price, M. N., Goodrich, J., Nawrocki, E. P., DeSantis, T. Z., Probst, A., Andersen, G. L., Knight, R., and Hugenholtz, P.: An improved Greengenes taxonomy with explicit ranks for ecological and evolutionary analyses of bacteria and archaea, ISMEJ, 6, 610-618, 10.1038/ismej.2011.139, 2012.

Mook, W.: Estuaries and the sea, in: Rozanski, K., Froehlich, K., Mook, W.G. (Eds.), Volume III: Surface Water, UNESCO, Paris, 49-56, 2001.

570 Nichols, P. D., Guckert, J. B., and White, D. C.: Determination of monosaturated fatty acid
571 double-bond position and geometry for microbial monocultures and complex consortia by
572 capillary GC-MS of their dimethyl disulphide adducts, J Microbiol Meth, 5, 49-55,
573 10.1016/0167-7012(86)90023-0, 1986.
574 Nichols, P. D., Skerratt, J. H., Davidson, A., Burton, H., and McMeekin, T. A.: Lipids of
575 cultured *Phaeocystis pouchetii*: Signatures for food-web, biogeochemical and environmental
576 studies in Antarctica and the Southern ocean, Phytochemistry, 30, 3209-3214, 10.1016/0031-
577 9422(91)83177-M, 1991.
578 Osburn, M. R., Sessions, A. L., Pepe-Ranney, C., and Spear, J. R.: Hydrogen-isotopic
579 variability in fatty acids from Yellowstone National Park hot spring microbial communities,
580 Geochim Cosmochim Ac, 75, 4830-4845, 10.1016/j.gca.2011.05.038, 2011.
581 Philippart, C., van Iperen, J., Cadée, G., and Zuur, A.: Long-term field observations on
582 seasonality in chlorophyll-a concentrations in a shallow coastal marine ecosystem, the Wadden
583 Sea, Estuaries and Coasts, 33, 286-294, 10.1007/s12237-009-9236-y, 2010.
584 Philippart, C. J. M., Cadee, G. C., van Raaphorst, W., and Riegman, R.: Long-term
585 phytoplankton-nutrient interactions in a shallow coastal sea: Algal community structure,
586 nutrient budgets, and denitrification potential, Limnol Oceanogr, 45, 131-144, 2000.
587 Pitcher, A., Wuchter, C., Siedenberg, K., Schouten, S., and Sinninghe Damsté, J. S.:
588 Crenarchaeol tracks winter blooms of ammonia-oxidizing Thaumarchaeota in the coastal North
589 Sea, Limnol Oceanogr, 56, 2308-2318, 10.4319/lo.2011.56.6.2308, 2011.
590 Quast, C., Pruesse, E., Yilmaz, P., Gerken, J., Schweer, T., Yarza, P., Peplies, J., and Glöckner,
591 F. O.: The SILVA ribosomal RNA gene database project: improved data processing and web-
592 based tools, Nucleic Acids Res, 10.1093/nar/gks1219, 2012.
593 Robins, R. J., Billault, I., Duan, J.-R., Guiet, S., Pionnier, S., and Zhang, B.-L.: Measurement
594 of ^{2}H distribution in natural products by quantitative ^{2}H NMR: An approach to understanding

595 metabolism and enzyme mechanism, Phytochem Rev, 2, 87-102,
596 10.1023/B:PHYT.0000004301.52646.a8, 2003.
597 Rütters, H., Sass, H., Cypionka, H., and Rullkotter, J.: Phospholipid analysis as a tool to study
598 complex microbial communities in marine sediments, J Microbiol Meth, 48, 149-160,
599 10.1016/s0167-7012(01)00319-0, 2002.
600 Sachs, J. P., Maloney, A. E., Gregersen, J., Paschall, C.: Effect of salinity on $^{2}H/^{1}H$ fractionation
601 in lipids from continuous cultures of the coccolithophorid *Emiliania huxleyi*, Geochim
602 Cosmochim Ac, 189, 96-109, 10.1016/j.gca.2016.05.041, 2016.
603 Saito, K., Kawaguchi, A., Okuda, S., Seyama, Y., and Yamakawa, T.: Incorporation of
604 hydrogen atoms from deuterated water and stereospecifically deuterium labeled nicotinamide
605 nucleotides into fatty acids with the *Escherichia coli* fatty acid synthetase system, Biochim
606 Biophys Acta, 618, 202-213, 1980.
607 Schloss, P. D., Westcott, S. L., Ryabin, T., Hall, J. R., Hartmann, M., Hollister, E. B.,
608 Lesniewski, R. A., Oakley, B. B., Parks, D. H., Robinson, C. J., Sahl, J. W., Stres, B.,
609 Thallinger, G. G., Van Horn, D. J., and Weber, C. F.: Introducing mothur: Open-source,
610 platform-independent, community-supported software for describing and comparing microbial
611 communities, Appl Environ Microbiol, 75, 7537-7541, 10.1128/aem.01541-09, 2009.
612 Schmidt, H.-L., Werner, R. A., and Eisenreich, W.: Systematics of ^{2}H patterns in natural
613 compounds and its importance for the elucidation of biosynthetic pathways, Phytochem Rev, 2,
614 61-85, 10.1023/B:PHYT.0000004185.92648.ae, 2003.
615 Schouten, S., Klein Breteler, W. C. M., Blokker, P., Schogt, N., Rijpstra, W. I. C., Grice, K.,
616 Baas, M., and Sinninghe Damsté, J. S.: Biosynthetic effects on the stable carbon isotopic
617 compositions of algal lipids: Implications for deciphering the carbon isotopic biomarker record,
618 Geochim Cosmochim Ac, 62, 1397-1406, 10.1016/S0016-7037(98)00076-3, 1998.

Sessions, A. L., Jahnke, L. L., Schimmelmann, A., and Hayes, J. M.: Hydrogen isotope fractionation in lipids of the methane-oxidizing bacterium *Methylococcus capsulatus*, Geochim Cosmochim Ac, 66, 3955-3969, 10.1016/s0016-7037(02)00981-x, 2002.

Sintes, E., Witte, H., Stodderegger, K., Steiner, P., and Herndl, G. J.: Temporal dynamics in the free-living bacterial community composition in the coastal North Sea, FEMS Microbiol Ecol, 83, 413-424, 10.1111/1574-6941.12003, 2013.

Sørensen, N., Daugbjerg, N., and Richardson, K.: Choice of pores size can introduce artefacts when filtering picoeukaryotes for molecular biodiversity studies, Microb Ecol, 65, 964-968, 10.1007/s00248-012-0174-z, 2013.

Vaezi, R., Napier, J. A., and Sayanova, O.: Identification and functional characterization of genes encoding omega-3 polyunsaturated fatty acid biosynthetic activities from unicellular microalgae, Marine Drugs, 11, 5116-5129, 10.3390/md11125116, 2013.

Valentine, D. L., Sessions, A. L., Tyler, S. C., and Chidthaisong, A.: Hydrogen isotope fractionation during H_2/CO_2 acetogenesis: hydrogen utilization efficiency and the origin of lipid-bound hydrogen, Geobiology, 2, 179-188, 10.1111/j.1472-4677.2004.00030.x, 2004.

Werner, J. J., Koren, O., Hugenholtz, P., DeSantis, T. Z., Walters, W. A., Caporaso, J. G., Angenent, L. T., Knight, R., and Ley, R. E.: Impact of training sets on classification of high-throughput bacterial 16s rRNA gene surveys, ISMEJ, 6, 94-103, 10.1038/ismej.2011.82, 2012.

Zhang, X. N., Gillespie, A. L., and Sessions, A. L.: Large D/H variations in bacterial lipids reflect central metabolic pathways, Proc Natl Acad Sci USA, 106, 12580-12586, 10.1073/pnas.0903030106, 2009a.

Zhang, Z., and Sachs, J. P.: Hydrogen isotope fractionation in freshwater algae: I. Variations among lipids and species, Org Geochem, 38, 582-608, 10.1016/j.orggeochem.2006.12.004, 2007.

643 Zhang, Z., Sachs, J. P., and Marchetti, A.: Hydrogen isotope fractionation in freshwater and
644 marine algae: II. Temperature and nitrogen limited growth rate effects, Org Geochem, 40, 428-
645 439, 10.1016/j.orggeochem.2008.11.002, 2009b.
646

647 **Figure and tables legends**

648 **Figure 1**

649 Values of $\varepsilon_{\Sigma FA}$ compared to chlorophyll *a* concentrations. $\varepsilon_{\Sigma FA}$ is the weighted average of
650 *n*C14:0, *n*C16:1, *n*C16:0, *n*C18:0 fatty acids and the *n*C20:5 PUFA from Jetty samples taken
651 from August 2010 – December 2011.

652 **Figure 2**

653 Phytoplankton diversity and abundance (measured in cells L^{-1}) observed in the coastal North
654 Sea between August 2010 – December 2011.

655 **Figure 3**

656 Order-level bacterial diversity and abundance in North Sea water based on the 16S rRNA gene
657 sequence.

658 **Figure 4**

659 Relative abundance of fatty acids and chlorophyll *a* concentration in North Sea SPM. (a)
660 *n*C14:0, (b) *n*C16:1, (c) *n*C16:0, (d) *n*C18:x, (e) *n*C18:0, (f) *n*C20:5 PUFA and chlorophyll *a.*

661 **Figure 5**

662 The D/H fractionation between fatty acids and North Sea water for fatty acids derived from
663 suspended particulate matter in North Sea water samples. Plotted are the the $\varepsilon_{lipid/water}$ values of
664 *n*C14:0, *n*C16:1, *n*C16:0, *n*C18:0 fatty acids and *n*C20:5 PUFA..

665 **Table 1**

666 D/H fractionation between fatty acids and North Sea water for fatty acids derived from
667 suspended particulate matter in North Sea water samples.

Table 1

Date	Salinity	δD_{water} [‰] (estimated)	$\varepsilon_{lipid/water}$ [‰]					$\varepsilon_{\Sigma FA}$ [‰]
			C14:0	C16:0	C16:1*	C18:0	C20:5 PUFA	weighted average C14, C16:1, C16, C18
16/08/10	27.3	-8.2	-212±2	-194±3	-194±3	-178±4	-185±2	-196±2
30/08/10	29.7	-4.1	-218±3	-198±3	-186±3	-182±2	-195±2	-197±2
15/09/10	30	-3.6	-213±3	-203±2	-194±2	-183±2	-177±3	-201±2
28/09/10	24.7	-12.6	-209±2	-188±2	-182±2	-187±2	-197±3	-190±2
15/11/10	30	-3.6	-211±3	-200±2	-179±2	-197±2	N.D.	-196±2
26/11/10	24.8	-12.4	-216±3	-192±3	-178±3	-193±3	N.D.	-193±2
10/12/10	27.1	-8.5	-218±2	-181±2	-184±2	-195±2	N.D.	-190±1
17/12/10	24.1	-13.6	-221±3	-182±2	-183±2	-177±3	N.D.	-188±2
10/01/11	27.8	-7.3	-215±4	-195±3	-180±2	-198±2	N.D.	-192±2
24/01/11	23.0	-15.5	-200±3	-179±2	-183±2	-180±2	-197±3	-183±2
17/02/11	29.3	-4.8	-219±2	-204±2	-191±2	-203±2	N.D.	-201±1
08/03/11	25.8	-10.7	-218±6	-206±3	-197±2	-173±4	-227±9	-202±2
23/03/11	26.8	-9.0	-234±2	-209±3	-198±2	-182±5	-234±2	-207±2
05/04/11	29.2	-4.9	-219±4	-206±5	-205±4	-208±6	-220±5	-208±2
19/04/11	27.7	-7.5	-229±2	-219±2	-215±2	N.D.	-235±2	-213±1
03/05/11	31.1	-1.7	-237±6	-224±2	-213±3	-210±3	-235±3	-223±2
18/05/11	31.8	-0.5	-219±2	-205±2	-197±3	-177±2	-213±2	-203±2
17/06/11	32.0	0.7	-225±3	-211±2	-196±4	-191±2	N.D.	-209±2
30/06/11	31.2	-1.6	-224±2	-208±2	-200±2	-173±7	-212±2	-209±2
15/07/11	30.0	-3.6	-202±2	-192±2	-185±2	-178±3	-215±3	-191±2
27/07/11	26.3	-9.9	-213±3	-192±3	-195±2	-172±2	-193±7	-194±2
08/08/11	29.4	-4.6	-219±7	-198±4	-197±5	-176±7	-231±4	-200±2
22/08/11	26.9	-8.9	-224±2	-195±2	-182±5	-183±3	-195±2	-199±2
06/09/11	26.8	-9.0	-217±6	-210±2	-213±4	-209±3	-211±3	-212±2
21/09/11	30.1	-3.4	-215±2	-201±2	-182±2	-191±3	N.D.	-198±1
11/10/11	32.8	1.2	-214±4	-192±2	-184±3	-189±4	-227±2	-194±2
28/10/11	32.2	0.1	-217±2	-188±2	-181±3	-184±2	-207±4	-190±2
15/11/11	28.9	-5.5	-208±12	-194±3	-187±5	-179±6	-217±2	-192±2
28/11/11	31.7	-0.7	-217±2	-192±2	-189±2	-180±3	-197±2	-195±1
16/12/11	31.7	-0.7	-198±7	-179±4	-173±5	-187±4	N.D.	-180±2

*n*C16:1*: double bond at the ω7 position

fig01

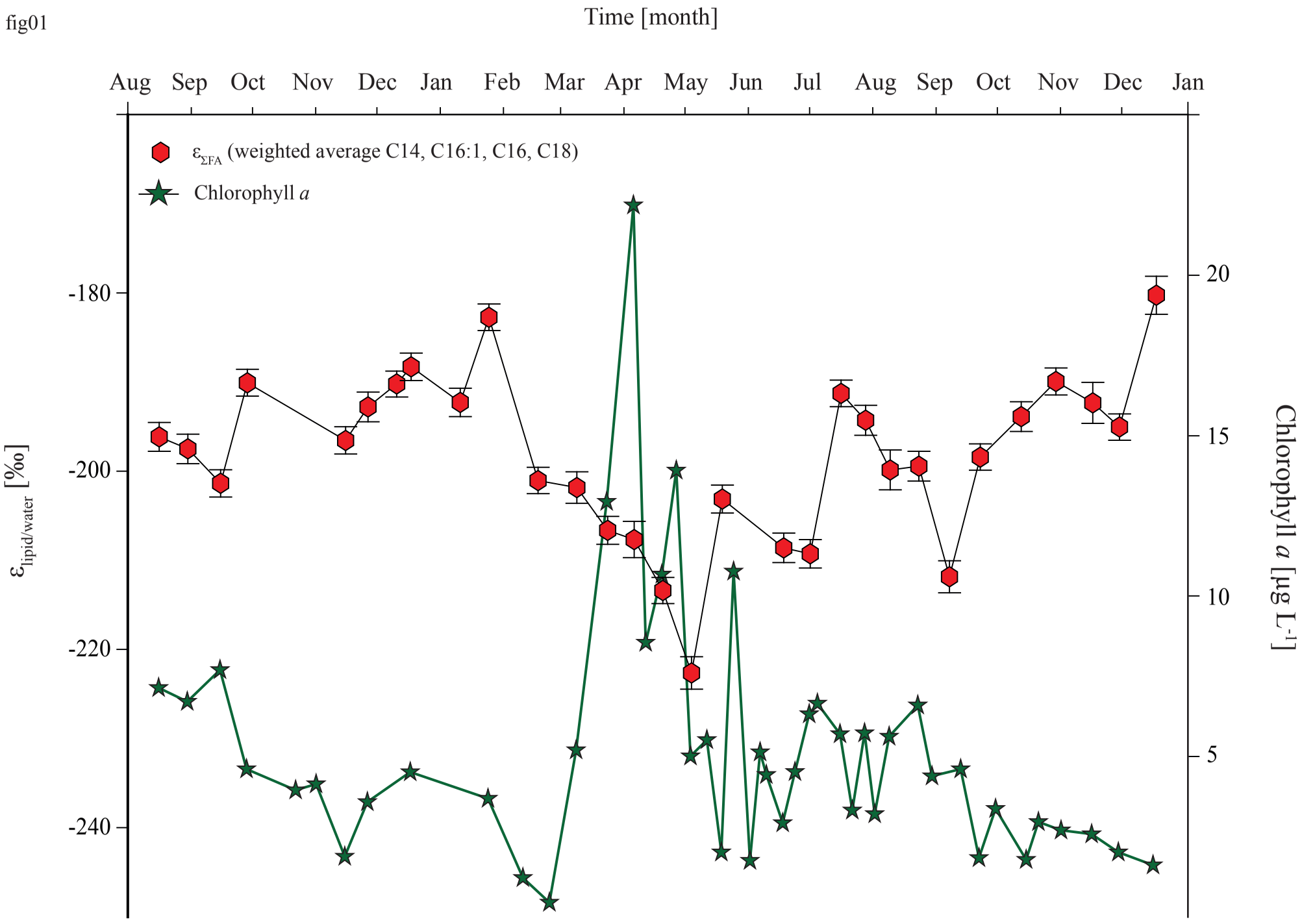
Time [month]
Aug
Sep
Oct
Nov
Dec
Jan
Feb
Mar
Apr
May
Jun
Jul
Aug
Sep
Oct
Nov
Dec
Jan
$\varepsilon_{\Sigma FA}$ (weighted average C14, C16:1, C16, C18)
Chlorophyll *a*
-180
-200
-220
-240
$\varepsilon_{lipid/water}$ [‰]
20
15
10
5
Chlorophyll *a* [µg L^{-1}]

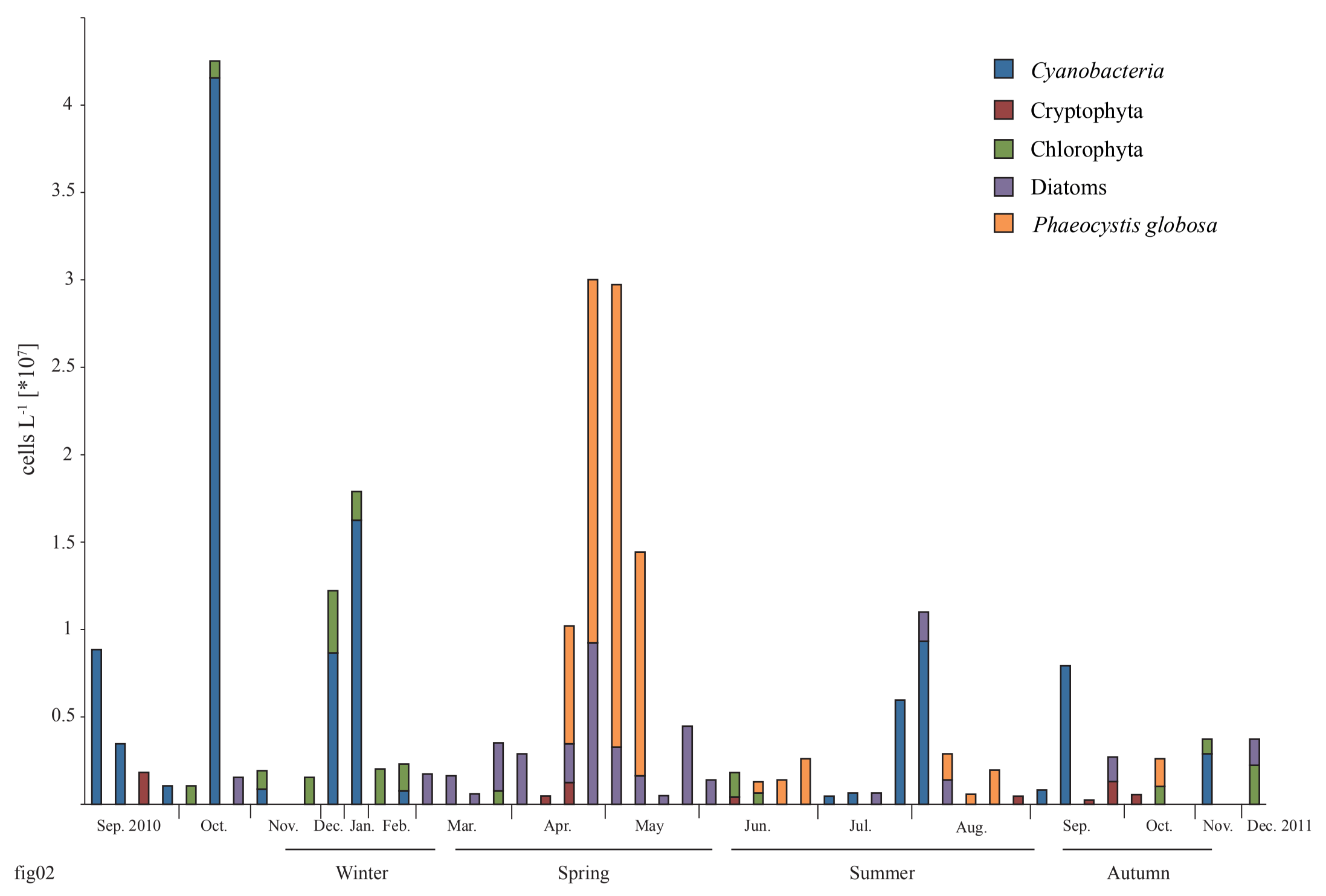
Cyanobacteria
Cryptophyta
Chlorophyta
Diatoms
Phaeocystis globosa
cells L-1 [*10^7]
4
3.5
3
2.5
2
1.5
1
0.5
Sep. 2010
Oct.
Nov.
Dec.
Jan.
Feb.
Mar.
Apr.
May
Jun.
Jul.
Aug.
Sep.
Oct.
Nov.
Dec. 2011
Winter
Spring
Summer
Autumn

fig02

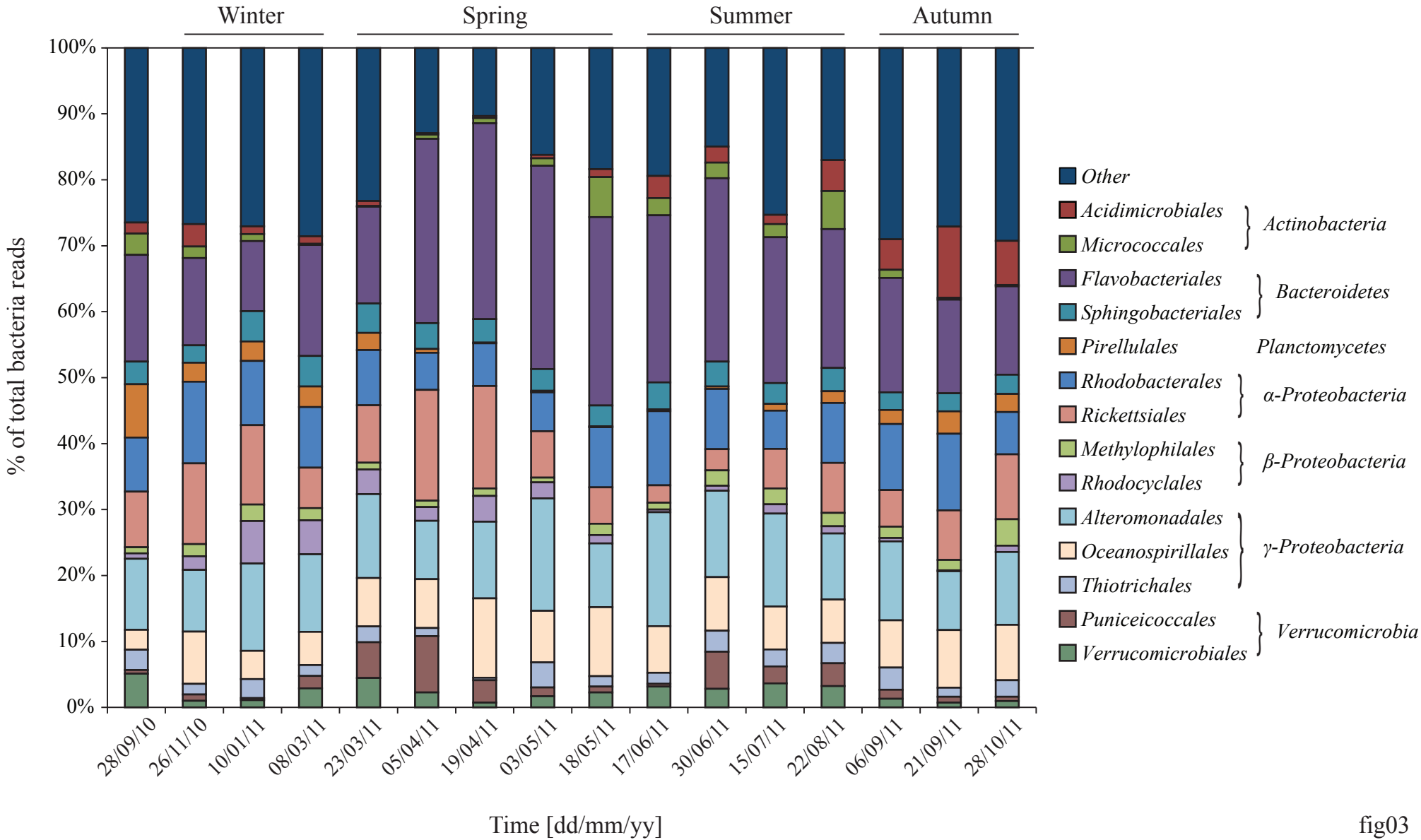
Winter
Spring
Summer
Autumn
100%
90%
80%
70%
60%
50%
40%
30%
20%
10%
0%
% of total bacteria reads
28/09/10
26/11/10
10/01/11
08/03/11
23/03/11
05/04/11
19/04/11
03/05/11
18/05/11
17/06/11
30/06/11
15/07/11
22/08/11
06/09/11
21/09/11
28/10/11
Time [dd/mm/yy]
Other
Acidimicrobiales
Micrococcales
Actinobacteria
Flavobacteriales
Sphingobacteriales
Bacteroidetes
Pirellulales
Planctomycetes
Rhodobacterales
Rickettsiales
α-Proteobacteria
Methylophilales
Rhodocyclales
β-Proteobacteria
Alteromonadales
Oceanospirillales
Thiotrichales
γ-Proteobacteria
Puniceicoccales
Verrucomicrobiales
Verrucomicrobia

fig03

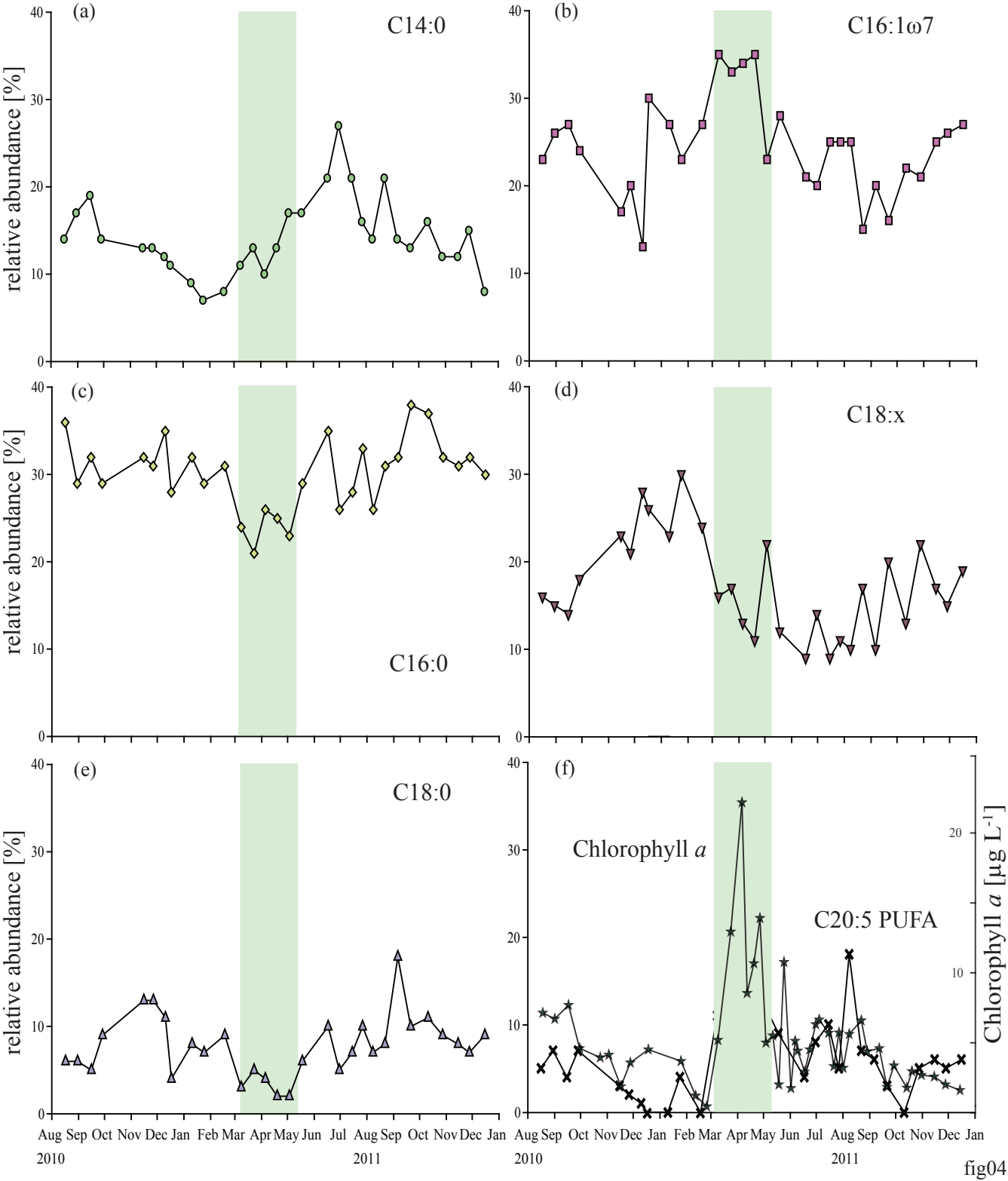
(a)
C14:0
(b)
C16:1ω7
(c)
C16:0
(d)
C18:x
(e)
C18:0
(f)
Chlorophyll a
C20:5 PUFA
relative abundance [%]
Chlorophyll a [µg L-1]
0
10
20
30
40
Aug Sep Oct Nov Dec Jan Feb Mar Apr May Jun Jul Aug Sep Oct Nov Dec Jan
2010
2011

fig04

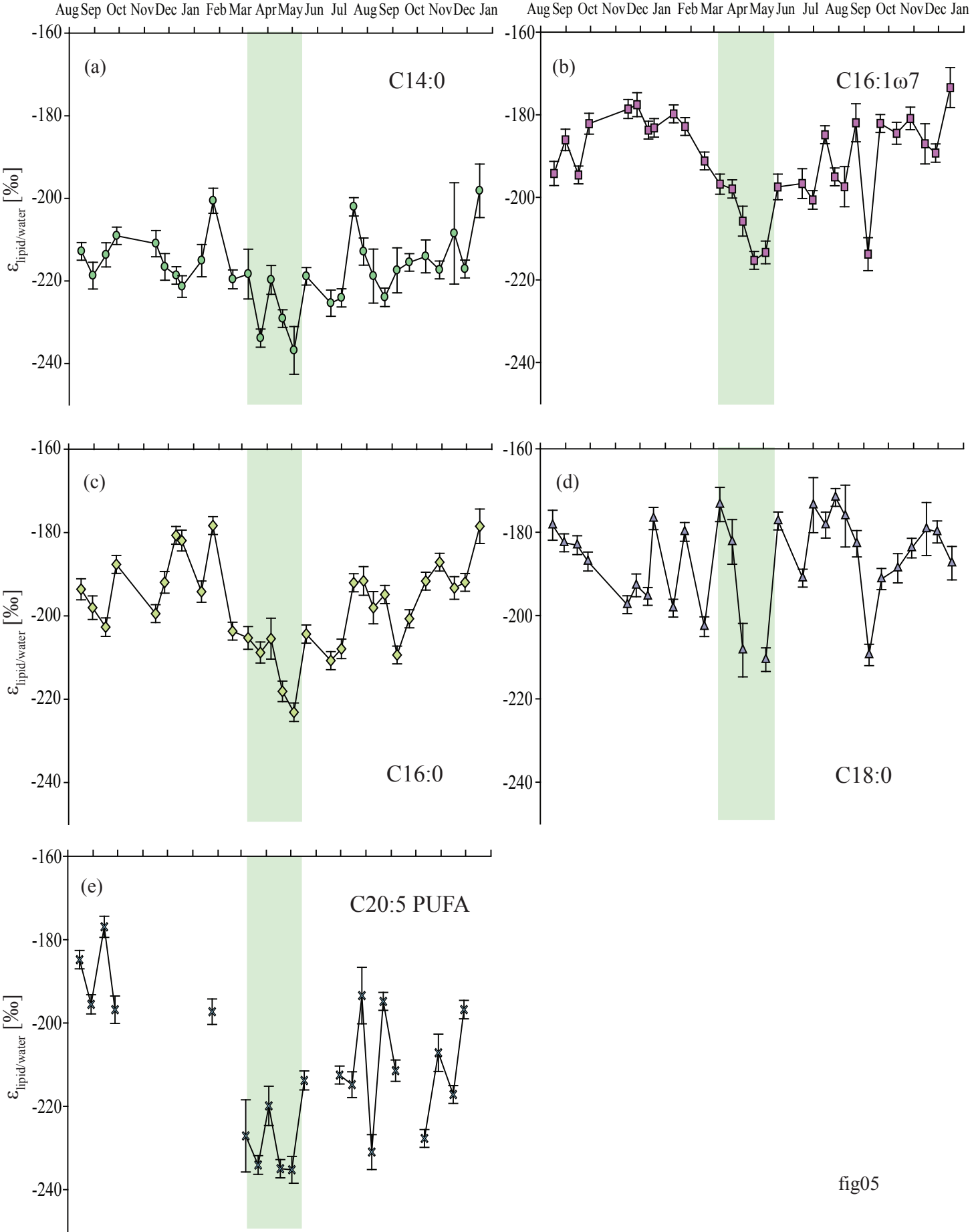
Aug Sep Oct Nov Dec Jan Feb Mar Apr May Jun Jul Aug Sep Oct Nov Dec Jan
(a)
C14:0
(b)
C16:1ω7
(c)
C16:0
(d)
C18:0
(e)
C20:5 PUFA
$\varepsilon_{lipid/water}$ [‰]
-160
-180
-200
-220
-240
fig05